Supramolecular Chemistry
Publication details, including instructions for authors and subscription information:
http://www.informaworld.com/smpp/title~content=t713649759

Polyazapodands Derived from Biphenyl. Study of their Behaviour as Conformationally Regulated Fluorescent Sensors

Ana M. Costero[a]; Joaquín Sanchis[a]; Salvador Gil[a]; Vicente Sanz[a]; M. Carmen Ramírez De Arellano[a]; J.A. Gareth Williams[b]
[a] Departament de Química Orgànica, Universitat de València, Burjassot, Spain [b] Department of Chemistry, University of Durham, Durham, UK

To cite this Article Costero, Ana M. , Sanchis, Joaquín , Gil, Salvador , Sanz, Vicente , De Arellano, M. Carmen Ramírez and Williams, J.A. Gareth(2004) 'Polyazapodands Derived from Biphenyl. Study of their Behaviour as Conformationally Regulated Fluorescent Sensors', Supramolecular Chemistry, 16: 6, 435 — 446
To link to this Article: DOI: 10.1080/10610270412331283574
URL: http://dx.doi.org/10.1080/10610270412331283574

Supramolecular Chemistry, September 2004, Vol. 16 (6), pp. 435–446

Taylor & Francis
Taylor & Francis Group

Polyazapodands Derived from Biphenyl. Study of their Behaviour as Conformationally Regulated Fluorescent Sensors

ANA M. COSTERO[a,*], JOAQUÍN SANCHIS[a], SALVADOR GIL[a], VICENTE SANZ[a], M. CARMEN RAMÍREZ DE ARELLANO[a] and J.A. GARETH WILLIAMS[b,†]

[a]*Departament de Química Orgànica, Universitat de València, C/Dr Moliner 50, 46100, Burjassot, Spain;* [b]*Department of Chemistry, University of Durham, South Road, Durham DH1 3LE, UK*

Received (in Southampton, UK) 5 April 2004; Accepted 15 June 2004

Eight new polyazapodands containing a 4,4′-substituted biphenyl moiety have been synthesised. Four (7, 8, 9 and 11) are functionalised on positions 4 and 4′ with a nitro group and four (1, 2, 3 and 10) with a dimethylamino substituent. Comparison of the emission behaviour of 1, 2, 3 with that of the reference compounds 10 and tetramthylbenzidine, clearly suggests that a modification in the dihedral angle between the biphenyl rings is an important factor in determining the fluorescent response of the molecule. The fluorescence is pH dependent, due to the formation of intramolecular hydrogen bonds between protonated aliphatic nitrogens and a carbonyl oxygen, which influences the aforementioned dihedral angle. A crystal structure resolved by X-ray diffraction of 7·2HCl has been determined, and confirms the dependence of the angle and the rigidity on the hydrogen bonding. The complexation properties of these ligands have been studied with Zn^{2+}, Cd^{2+}, Ni^{2+}, Cu^{2+} and Pb^{2+}, which show that the number of amino groups within the pendants has a strong influence on the nature of the complexation and the fluorescent response of each ligand.

Keywords: Tetramethylbenzidine; Conformational regulation; Fluorescent sensors

INTRODUCTION

Our research group has been interested for several years in the preparation of ligands containing in their structure the 4,4′-bis(dimethylamino)biphenyl (TMB = tetramethylbenzidine) subunit. The electrochemical properties of the TMB system have been widely studied [1–4], and the parent compound and several derivatives have been used in the generation and study (by electron spin resonance) of the corresponding radical cations [5]. However, the fluorescent properties of these systems have received less attention. Nevertheless, a clear relationship has been established between the fluorescence properties of biphenyl derivatives and the dihedral angle formed between the two aromatic rings [6]. This conformational dependence of the emission has been used in the design of several fluorescent chemosensors [7,8]. Our previous results have demonstrated that TMB can be incorporated successfully into several such systems [9,10]. The previously studied ligands contain a coronand unit directly bound to the 2,2′-positions of the biphenyl system and, as a consequence of their structure, the modification of the dihedral angle between the two aromatic rings is restricted. Now, we report on the synthesis of several related podand ligands that can widely modify their conformation by rotation around the bond between the aromatic rings (Chart 1). In addition, these new ligands contain a variable number of nitrogen atoms to modulate the transition metal cation complexation. Finally, the presence of amide substituents gives additional information about the influence of the dihedral angle in the fluorescent behaviour, because the presence of these carbonyl groups can give rise, in some cases, to hydrogen bonding that fixes, even more rigidly, the dihedral angle between the aromatic rings.

*Corresponding author. Tel.: +34-96-354-4410. Fax: +34-96-354-3152. E-mail: ana.costero@uv.es
†E-mail: j.a.g.williams@durham.ac.uk

ISSN 1061-0278 print/ISSN 1029-0478 online © 2004 Taylor & Francis Ltd
DOI: 10.1080/10610270412331283574

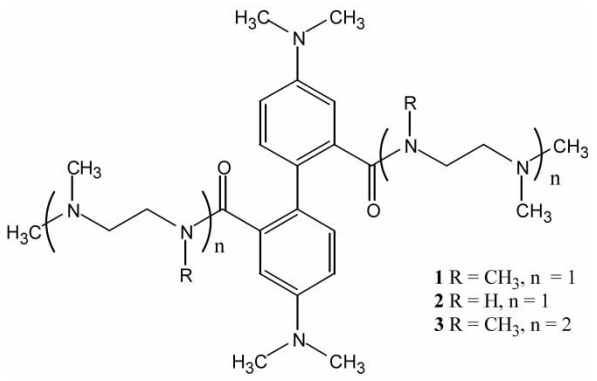

CHART 1

SYNTHESIS AND CONFORMATIONAL STUDIES

Compounds **1**–**3** were synthesised as shown in Scheme 1. Treatment of 4,4′-dinitro-2,2′-diphenic acid with thionyl chloride gave the corresponding dichloride derivative. The reaction of this compound with the corresponding polyamines **4**–**6** provided compounds **7**–**9**, which were converted into **1**–**3**, respectively, by reaction with formaldehyde under reducing conditions (H_2, Pd(C)) [11]. In addition, compound **10** was prepared for use in control experiments.

Amines **4** and **5** are commercially available. Compound **6**, in contrast, was prepared following the pathway described in Scheme 2. Thus, *N*-methylethanolamine was converted into its ditosyl derivative **12** following a previously described procedure [12]. Reaction of compound **12** with trimethylethylenediamine in the presence of NaI gave rise to compound **13** in only one step, and with higher yields than those obtained following earlier procedures described for preparing similar compounds [13]. Finally, **6** was obtained by treatment of **13** with concentrated sulphuric acid [14].

The prepared ligands have two amide units, and three conformational isomers are, in principle, possible: *cisoid–cisoid*, *transoid–cisoid* and *transoid–transoid* (Chart 2). Ligands **2** and **8** have two amide NH units; their ^{1}H NMR spectra show the expected multiplicity of signals for their methylene groups. Their ^{13}C NMR spectra show single peaks for each chemically equivalent carbon, indicating a symmetrical structure and lack of conformational isomerism. The appearance of a downfield NH signal for these compounds is indicative of a CO···HN intramolecular hydrogen bond, involving a carbonyl group on one chain and the amidic hydrogen on the other.

Ligands **1**, **3**, **7** and **9**, on the other hand, show different aliphatic N—CH_3 signals and several sets of aromatic signals in their ^{1}H NMR spectra. Clearly, therefore, the presence of the relatively bulky methyl substituents on the amidic nitrogens in these compounds leads to restricted rotation around the amide bonds and generates different conformations.

Compound **1**·2HCl shows, by ^{1}H NMR, three possible conformations in CD_3OD, because three different $N(CH_3)_2$ signals are observed for the aliphatic amine group. The signals corresponding to two of the conformations are very similar,

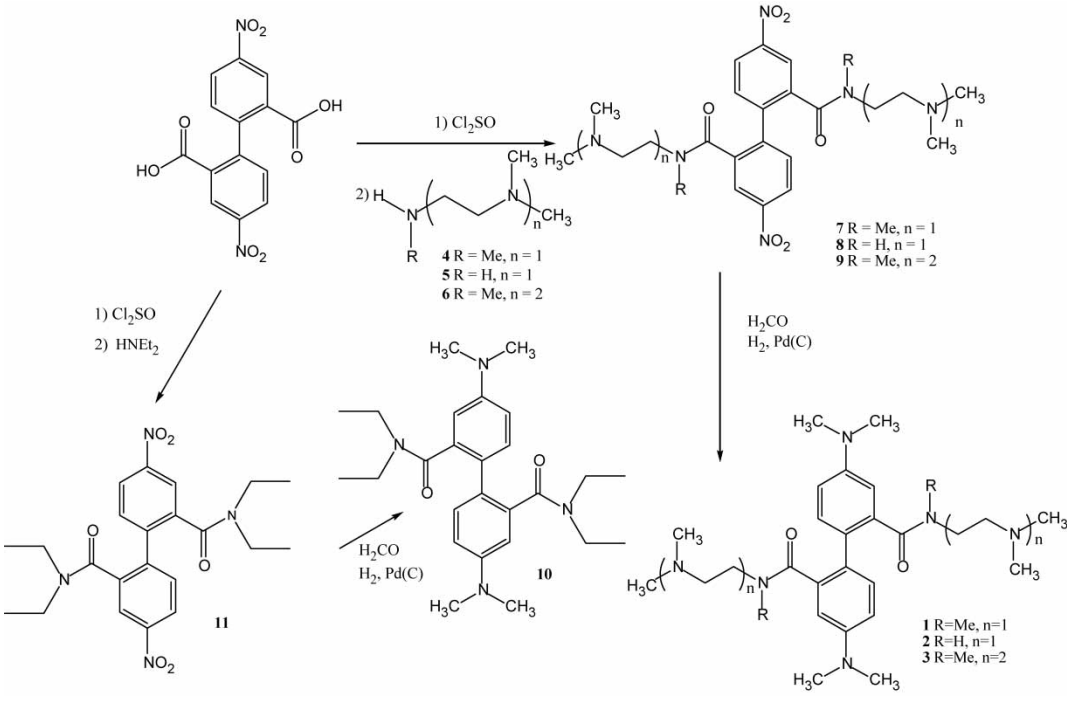

SCHEME 1

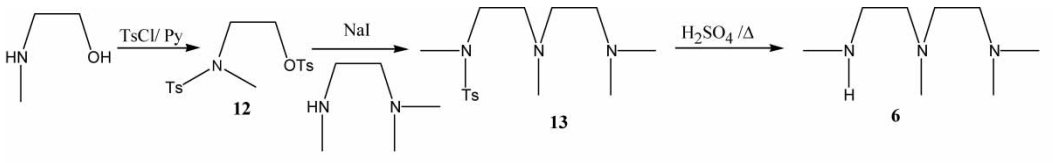

SCHEME 2

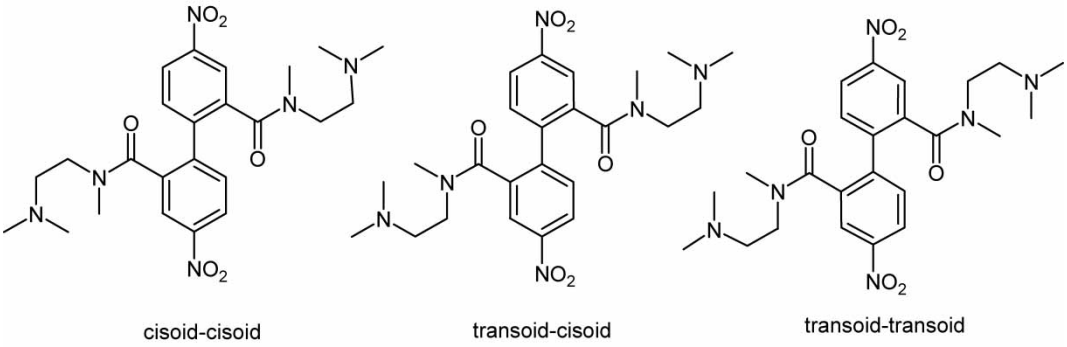

CHART 2

however, and so it is only possible to establish the proportion of the major conformation compared to the mixture of the other two. This ratio was around 2.5:1.

Compound **7**·2HCl shows two possible conformations under the same conditions. Two different methyl signals are observed for the aliphatic amine groups and also two different ones for the methyl attached to the amidic nitrogen. The equilibrium ratio between these two conformations is approximately 4:1. Additionally, most of the signals in the corresponding ^{13}C NMR spectrum are duplicated. NMR spectroscopic studies of ligands **1** and **7** were also carried out in other solvents (CD_3CN and $CDCl_3$), and the results obtained demonstrated that the proportions of the different conformers were strongly solvent dependent.

On the other hand, a much more complex situation was observed with ligands **3**·2HCl and **9**·2HCl. In these cases, up to four conformations were detected in CD_3OD. Unfortunately the relative proportions could not be determined due to the complexity of the spectra, although, again, a strong solvent dependence was observed.

X-RAY DETERMINATIONS

A single crystal of ligand **7**, as its dichlorohydrate, could be obtained in the presence of HgI_2 (Fig. 1). Thus, crystallisation of an ionic pair by slow liquid–liquid diffusion was achieved in an H-shaped tube. The crystal structure of compound **7** shows a dicationic macromolecule and two independent dimeric $[Hg_2I_6]^{2-}$ and $[Hg_2I_4Cl_2]^{2-}$ half anions. Analysis of the dication structure indicates that **7** is present in the crystal structure in the *cisoid–transoid* conformation [O(2)-C(7)-N(3)-C(8) 1.0(15)°, O(1)-C(1)-N(1)-C(2) 13.4(14)°]. Both of the ammonium N—H bonds act as hydrogen bond donors, one forming an intramolecular N—H···O hydrogen bond [N(2)···O(2) 2.761(12), H(2)···O(2) 1.88 Å, N(2)-H(2)···O(2) 163.0°] and the other, an intermolecular N—H···Cl hydrogen bond [N(4)···Cl(5) 3.392(10), H(4)···Cl(5) 2.63 Å, N(4)-H(4)···Cl(5) 141.1°]. Thus, the apparently "more energetic" *cisoid* conformation is then stabilized by the hydrogen-bond. The dihedral angle between the phenyl aromatic

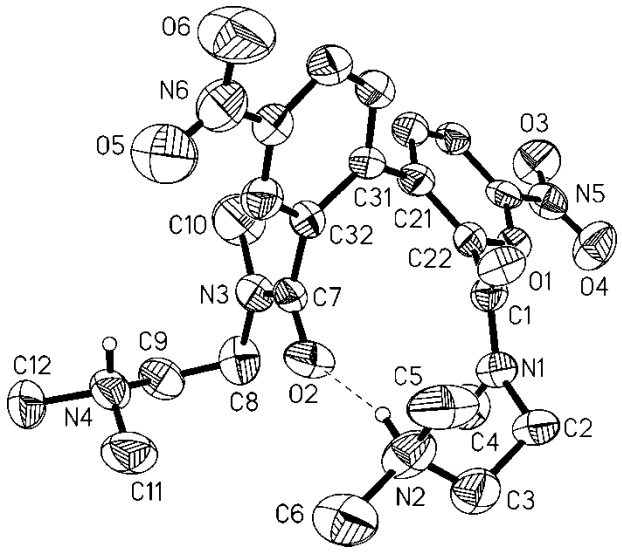

FIGURE 1 Ellipsoid plot (50% probability) of the cation of compound **7**, showing the molecular labelling. Hydrogen atoms have been omitted for clarity (except NH).

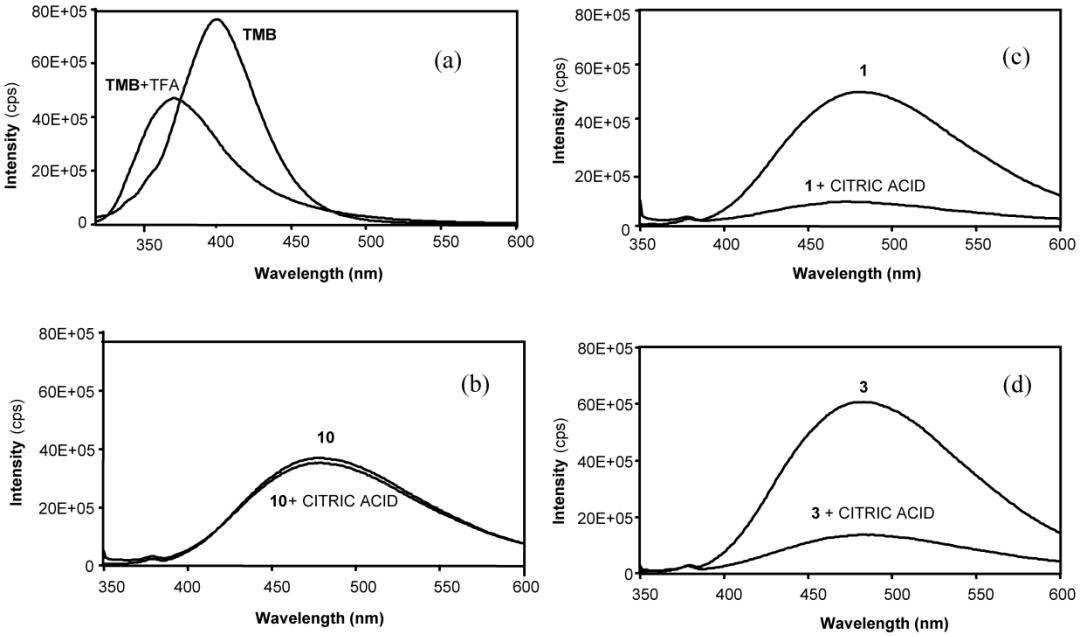

FIGURE 2 Fluorescence spectra under neutral and acidic conditions at 20°C: (a) TMB and TMB + TFA: $\lambda_{exc} = 310$ nm, initial concentration of TMB was 6.37×10^{-7} M. TFA was added in a large excess; (b) reference compound **10** and **10** + citric acid: $\lambda_{exc} = 340$ nm, initial concentration of **10** was 4.73×10^{-6} M, final concentration of citric acid was 4.25×10^{-4} M; (c) **1** and **1** + citric acid: $\lambda_{exc} = 340$ nm, initial concentration of **1** was 5.92×10^{-6} M, final concentration of citric acid was 6.39×10^{-5} M; (d) **3** and **3** + citric acid: $\lambda_{exc} = 340$ nm, initial concentration of **3** was 4.90×10^{-6} M, final concentration of citric acid was 2.39×10^{-4} M.

rings is 64° [C(32)-C(31)-C(21)-C(22) 63.6(13)°]. It is also noteworthy that there is a certain distortion in the hypothetical tetrahedral angles of the atoms in the aliphatic chains, this effect being larger in the *transoid* branch than in the *cisoid* one [N(3)-C(8)-C(9) 115.0(10)°, C(9)-N(4)-C(11) 118.0(11)° for the *transoid* and N(1)-C(2)-C(3) 113.1(9)°, C(5)-N(2)-C(3) 114.7(11)° in the *cisoid*]. In both $[Hg_2I_6]^{2-}$ and $[Hg_2I_4Cl_2]^{2-}$ dimers, the metallic moieties are symmetry related by an inversion centre in the Hg···Hg midpoint. In the dimers, the mercury atoms present a tetrahedral geometry with two asymmetrically bridging iodine atoms [Hg(1)-I(1) 2.8422(9), Hg(1)-I(1)^{i} (*i*: $-x$, $1-y$, $1-z$) 2.9426(10), Hg(2)-I(4) 2.9319(15), Hg(2)-I(4)^{ii} (*ii*: $2-x$, $2-y$, $-z$) 2.8033(14) Å].

UV AND FLUORESCENT PROPERTIES

Theoretical calculations indicate that the presence of substituents in the 2 and 2′ positions of the TMB unit modifies the dihedral angle between the two aromatic rings (from 38.7° in TMB itself to 56.9, 74.9, 63.3 and 57.1° in **1**, **2**, **3** and **10**, respectively)[‡]. Steric repulsions and, in compound **2**, intramolecular hydrogen bond formation, account for this. Due to these modifications, clear perturbations are observed not only in absorption, but also in the fluorescence emission spectra of the prepared ligands (Fig. 2). Thus, the absorption band at 310 nm in TMB is shifted to 290, 280, 295 and 294 nm for **1**, **2**, **3** and **10**, respectively (Table I). The blue shift observed for these ligands, relative to the model compound, seems to be related to modification of the mean dihedral angle between the aromatic rings that hinders the extension of the conjugation in the excited state. On the other hand, the fluorescence properties of the prepared ligands show clear modifications in relation to the parent compound which agree with previous observations about

TABLE I UV-absorption and fluorescence emission parameters in solution in CH_3CN at 20°C. τ_{exc} for TMB = 310 nm and λ_{exc} for **1**,**2**,**3** and **10** was 340 nm. Estimated uncertainty in lifetimes ± 0.2 ns. Quantum yields were determined using quinine sulphate in 1 M H_2SO_4 as the standard, estimated uncertainty ± 20%

Ligand	$\lambda_{absorption}$ nm/(ε/cm^{-1}M^{-1})	$\lambda_{emission}$ /nm	Φ	Lifetime /ns
TMB	310 (34668)	401	0.043	11.6
1	290 (18180)	482	0.041	2.0
2	280 (15338)	473	0.035	3.1
3	295 (23059)	483	0.035	2.1
10	294 (27306)	478	0.041	2.3

[‡]Optimisation of geometry was performed by Molecular Mechanics using MMX as Force Field contained in Pcmodel for Windows. V. 8.00.1, June 14, 2001. Serena software. http://www.serenasoft.com

the influence of the dihedral angle in the fluorescent properties of biphenyl derivatives [6,10]. The fluorescence spectra of the present compounds show an emission band which is always at longer wavelength than that of TMB [15] (Table I). The quantum yields of emission and the fluorescence lifetimes of these compounds have also been measured, and their values are reported in Table I.

Effect of Protonation

The fluorescent properties of the new ligands are strongly dependent upon the hydrogen ion concentration (*i.e.* the protonation state). The dimethylamino groups in the TMB systems are only weakly basic and, for that reason, are only protonated in the presence of relatively strong acids, such as trifluoroacetic acid (TFA). Protonation of the dimethylamino group under these conditions leads to a substantial blue-shift in the emission spectrum to 373 nm, and a slightly reduced quantum yield compared to that of TMB (Fig. 2a). Weaker acids (*e.g.* citric acid) are unable to protonate the dimethylaniline groups, and no modification of the emission spectrum is observed in the presence of an excess of such acids. Similarly, the fluorescence of the control compound **10** is not affected by citric acid, ruling out any additional effect due to the amide substituents under these conditions (Fig. 2b). In complete contrast, when ligands **1** and **3** were studied in the presence of citric acid, a substantial quenching of the fluorescence is observed (Fig. 2c and d). A possible explanation for this behaviour may lie in the formation of intramolecular hydrogen bonds under the acidic conditions. Thus, the presence of hydrogen bond interactions between the carbonyl group of one chain and a protonated amine group in the other could influence the dihedral angle, perhaps locking the system into a conformation that is more susceptible to non-radiative deactivation and thereby lowering the emission intensity. This suggestion agrees with the results obtained with ligand **2**. The presence of a NH group in ligand **2** gives rise to a permanent hydrogen bond between this hydrogen and the carbonyl group in the opposite branch. Thus, this ligand already has a rigid structure with a fixed dihedral angle between both aromatic rings, and protonation induces a smaller change in its geometry than occurs in ligands **1** and **3**. This explains the differences in quenching observed for ligands **1** and **3** (around 70%) when compared with ligand **2** (20%).

COMPLEXATION STUDIES

Complexation studies of ligands **1**, **2**, **3** and **10** with several transition metal cations (Cu^{2+}, Cd^{2+}, Zn^{2+}, Pb^{2+}, and Ni^{2+}) were carried out in acetonitrile.

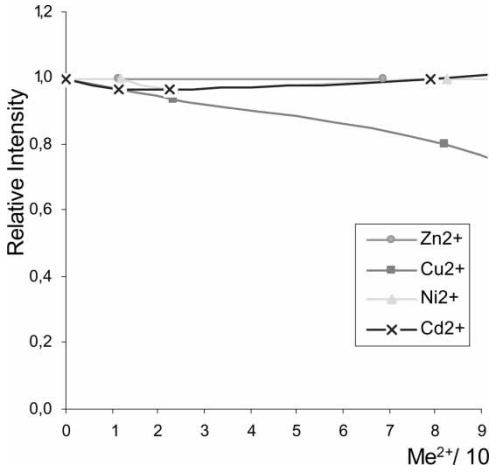

FIGURE 3 Relative intensity of emission of fluorescence ($\lambda_{exc} = 340$ nm) in titration of **10** with different divalent metals in acetonitrile, 20°C. Initial concentration of **10** was *ca.* 3.6×10^{-6} M, of TMAOH 7.2×10^{-6} M and of $TBAPF_6$ was 1×10^{-4} M.

Experiments were initially undertaken with the control compound **10** (Fig. 3) and with TMB (Fig. 4), monitoring the UV-visible and fluorescence spectra as a function of increasing metal ion concentration. Note that in Figs. 3–10, the *x*-axis refers to the mole ratio of the metal ion to the ligand under investigation. With the exception of Cu^{2+}, no significant changes in the spectra were observed. This helps to confirm that neither the amide groups nor the dimethylamino substituents present in these ligands are suitable for complexing transition metal cations. Copper led to partial quenching of the fluorescence emission, but intermolecular diffusion-controlled quenching of fluorophores by Cu^{2+} is commonplace, and does not require any specific binding of the metal ion (some weak interaction with the dimethylamino units cannot be ruled out, however). The behaviour of **1**, **2** and **3**, on the other hand, is in striking contrast to that of the control

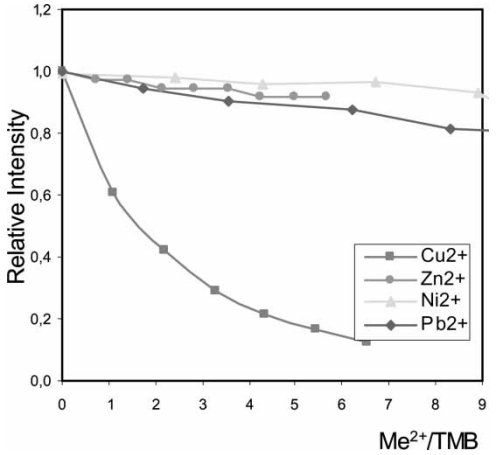

FIGURE 4 Relative intensity of emission of fluorescence ($\lambda_{exc} = 310$ nm) in titration of TMB with different divalent metals in acetonitrile, 20°C. Initial concentration of TMB was *ca.* 1×10^{-6} M, no extra base was added.

TABLE II Complexation constants (M^{-1}) of 1:1 (L:M) complex formation for ligands **1**, **2** and **3** in acetonitrile at 20°C. All metal salts were triflates. Error bars were in all cases, less than 10%

Ligand	Cu^{2+}	Zn^{2+}	Cd^{2+}	Ni^{2+}	Pb^{2+}
1	$2.34\ 10^4$	$2.46\ 10^4$	$1.95\ 10^4$	$1.95\ 10^4$	$1.37\ 10^4$
2	$3.40\ 10^4$	$3.75\ 10^4$	$2.70\ 10^4$	$2.70\ 10^4$	$2.43\ 10^4$
3	$2.45\ 10^4$	$2.30\ 10^{4*}$	$3.85\ 10^{2*}$	$4.93\ 10^4$	$1.83\ 10^4$

*This constant refers to a stoichiometry LM_2, (M^{-2}).

compounds. These three ligands showed marked perturbations of their fluorescence spectra upon addition of the metal ions which, given the lack of response by the control compounds, must clearly be associated with complexation by the aliphatic amine groups in these ligands. Association constants for the cations (as triflate salts) were determined by titration experiments using the intensity of the emitted fluorescence as a linearly variable property and by fitting the data to the model described below (details are given in the experimental section). The values obtained are shown in Table II. Most of the complexes displayed a 1:1 binding stoichiometry, and only **3**·Cd^{2+} and **3**·Zn^{2+} showed a different behaviour (see later). From the experimental behaviour of the emission in the titrations, and the calculated stoichiometries, the following model of interaction between ligand and cation can be proposed. Thus, ligand **1** displays a quenching of emission intensity of around 90% after the addition of one equivalent of metal ion, with remarkably little dependence on the identity of the metal (Fig. 5).

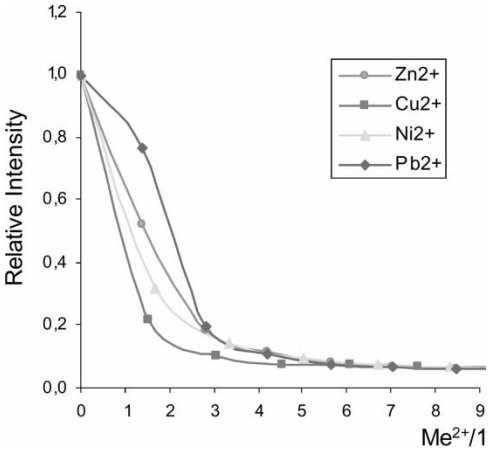

FIGURE 5 Relative intensity of emission of fluorescence ($\lambda_{exc} = 340$ nm) in titration of **1** with different divalent metals in acetonitrile, 20°C. Initial concentration of **1** was *ca.* 6×10^{-6} M, of TMAOH 1.3×10^{-5} M and of $TBAPF_6$ was 1×10^{-4} M.

Given the 1:1 (L:M) stoichiometry of binding, the most likely geometry of complex formation is form (a) in Chart 3, in which both chains are involved in binding to the metal. The hindrance that such complexation may impart on the rotation of the two phenyl rings relative to one another may explain the quenching of the fluorescence observed in the presence of the metal ions, and the similar behaviour found for each of the metals investigated. Such an explanation is supported by results with ligand **2**, which has a similar structure but with an amidic proton which can be removed by a suitable base. The behaviour of **2** with metals has been studied under different acid–base conditions (Figs. 6 and 7). For instance, in the case of Zn (Fig. 8), which is a post-transition metal with no ligand field stabilization energy effects, complexation of the metal is not sufficiently favourable, energetically, to be accompanied by removal of the amidic hydrogen. Therefore when no base is present in the medium, **2** interacts with Zn in the same way as ligand **1** does (Chart 3, form (a)) giving 80% quenching. When an excess of base (tetrabutylammonium hydroxide) is added, the amidic hydrogen is removed and, in that situation, Zn is chelated by both nitrogens of the same branch (Chart 3, form (b)). This disposition does not constrain the torsion angle between

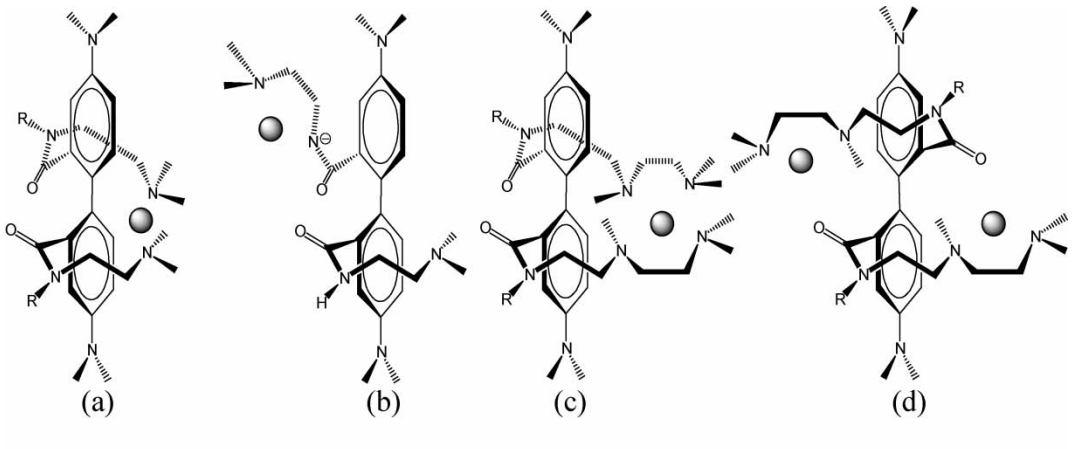

CHART 3 Possible complexing arrangements, suggested to explain the fluorescence results, for the different ligands and cations. Solvent molecules, supposed to complete coordination sites, have been avoided for clarity.

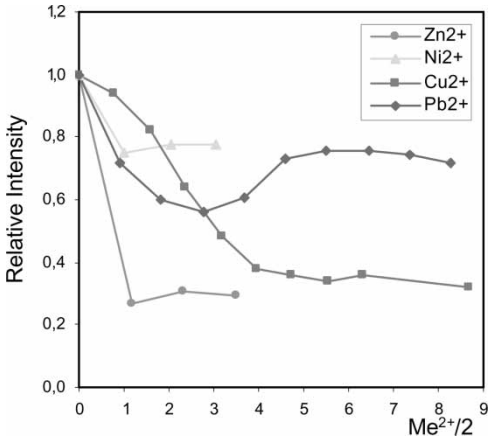

FIGURE 6 Relative intensity of emission of fluorescence ($\lambda_{exc} = 40$ nm) in titration of **2** with different divalent metals in acetonitrile, 20°C. Initial concentration of **2** was *ca.* 3×10^{-5} M, no extra base was added.

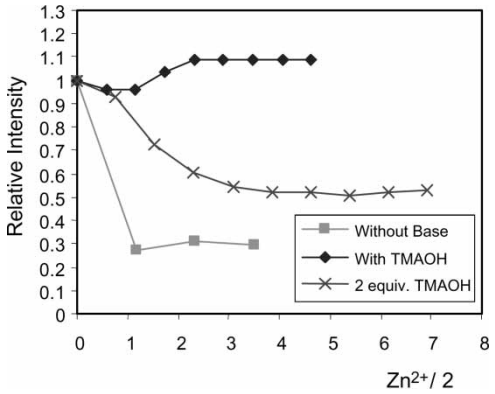

FIGURE 8 Relative intensity of emission of fluorescence ($\lambda_{exc} = 340$ nm) in titration of **2** with Zn^{2+} in acetonitrile, 20°C. (a) Initial concentration of **2** was 1.6×10^{-5} M. (b) Initial concentration of **2** was 3.5×10^{-5} M and there was an excess of TMAOH before addition of metal. (c) Initial concentration of **2** was 5.2×10^{-6} M, TMAOH 1×10^{5} M and of $TBAPF_6$ was 1×10^{-4} M.

the biphenyls, so that quenching is not induced. If only 2 equiv. of base are added, the basicity of the medium is not strong enough to remove quantitatively the proton, and an intermediate situation occurs. On the contrary, for Ni (Fig. 9), the formation of the chelated form with **2** is now favoured by ligand field stabilization such that the amide proton is removed without additional base being required, and similar spectra are therefore observed with or without base.

Ligand **3** exhibits more interesting results in complexation experiments, with two distinct binding stoichiometries possible, depending on the identity of the metal ion. Thus, Cu^{2+}, Ni^{2+}, and Pb^{2+} gave a 1:1 complex, even in the presence of high concentrations of the cation. Quenching of the fluorescence was observed in each case (Fig. 10), with a considerable shift of the wavelength of the emission maximum for Cu^{2+} and Pb^{2+}, and the association constants were similar to those determined for ligands **1** and **2**. It is reasonable, therefore, to propose a complex geometry in which both amino chains are involved in complexation (form (c) in Chart 3). As suggested above, the constraining influence of such a coordination mode on rotation within the biphenyl moiety may be the source of the fluorescence quenching. In contrast, addition of Cd^{2+} and Zn^{2+} leads, initially, to a quenching of the fluorescence and accompanying red-shift, but subsequently to an enhancement of the intensity in the presence of higher concentrations of the metal ions (Fig. 11), to the extent that the original intensity is finally restored. Mole ratio plots [16] of the titration data of **3** with Zn^{2+} and Cd^{2+} showed the formation of a 1:2 complex under these conditions (Fig. 12). One possible explanation for this different fluorescent behaviour can be found in the formation of a 1:2 complex (form (d) in Chart 3), in which each amino

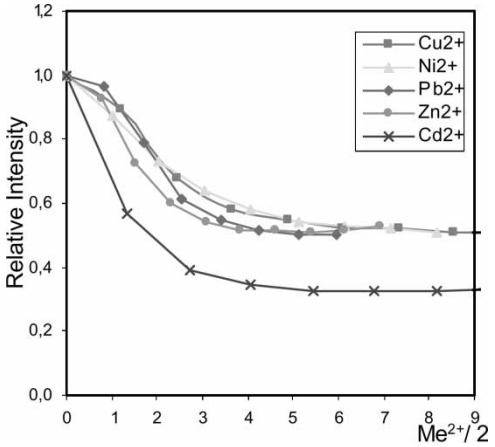

FIGURE 7 Relative intensity of emission of fluorescence ($\lambda_{exc} = 340$ nm) in titration of **2** with different divalent metals in acetonitrile, 20°C. Initial concentration of **2** was *ca.* 5×10^{-6} M, of TMAOH 1×10^{-5} M and of $TBAPF_6$ was 1×10^{-4} M.

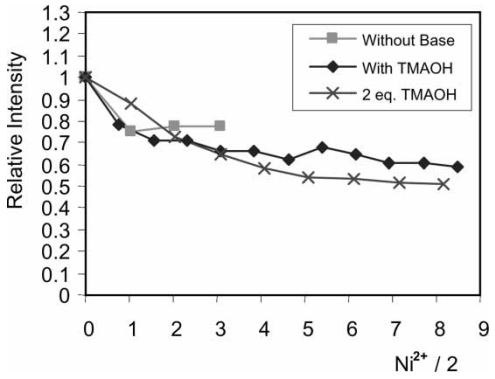

FIGURE 9 Relative intensity of emission of fluorescence ($\lambda_{ex} = 340$ nm) in titration of **2** with Ni^{2+} in acetonitrile, 20°C. (a) Initial concentration of **2** was 2.5×10^{-5} M. (b) Initial concentration of **2** was 3×10^{-5} M and there was an excess of TMAOH before addition of metal. (c) Initial concentration of **2** was 4.7×10^{-6} M, TMAOH 1×10^{-5} M and of $TBAPF_6$ was 1×10^{-4} M.

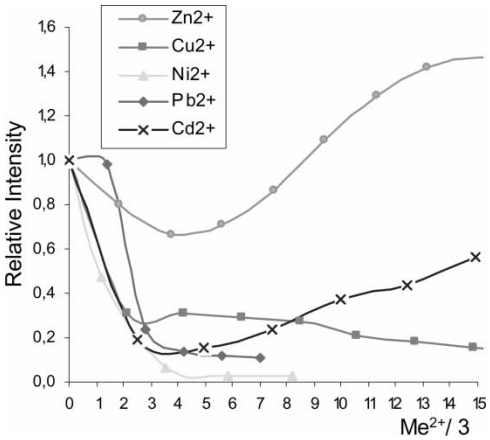

FIGURE 10 Relative intensity of emission of fluorescence ($\lambda_{exc} = 340$ nm) in titration of **3** with different divalent metals in acetonitrile, 20°C. Initial concentration of **3** was *ca.* 4.4×10^{-6} M, of TMAOH 1.4×10^{-5} M and of $TBAPF_6$ was 1×10^{-4} M.

chain is involved in complexing one cation only. Taking into account that both cations cannot quench by themselves, this newly generated open geometry could explain the restoration of the fluorescence at high concentrations, because such a complex will be more flexible than the folded system with 1:1 stoichiometry and the dihedral angle will no longer be constrained by hydrogen bonding or inter-chain cation coordination.

CONCLUSIONS

Eight new ligands containing the 4-4′-bis(dimethylamino)-biphenyl unit have been prepared by reduction of the corresponding nitro-substituted compounds. The compounds also contain amide groups in the 2 and 2′ positions, carrying potentially coordinating amino pendants.

Rotation within the amide branches is restricted, because of the amide moiety, as evident from

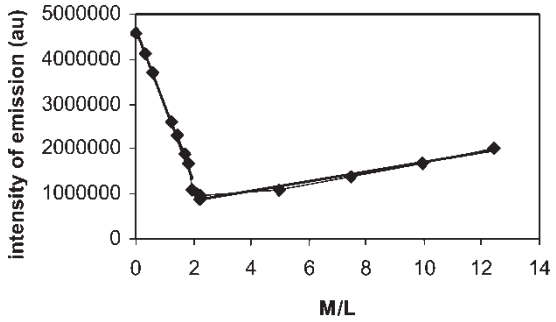

FIGURE 12 Mole ratio plot [17] applied to titration of **3** with Cd^{2+} in CH_3CN at 20°C. Variable property was the intensity at the fluorescence emission maximum. $\lambda_{exc} = 340$ nm.

the strong dependence of the ^1H NMR spectrum on the pH and the solvent. Ligands **1**, **2**, **3** and **10** are fluorescent, with emission maxima around 470 nm and quantum yields of about 0.04. Under mildly acidic conditions (citric acid), compounds **1**, **2** and **3** experience a considerable fluorescence quenching, but not the control compound **10**, a tertiary amide which lacks amide or amine N—H bonds. Formation of an intramolecular hydrogen bond between a protonated aliphatic nitrogen and the carbonyl oxygen probably changes and restricts the dihedral angle of the biphenyl group, leading to the observed effect on the excited state of the fluorophore. This hypothesis is supported by a similar arrangement in the crystal structure of **7**·2HCl. Ligand **1** binds a variety of transition and post-transition metal ions, signalled by fluorescence quenching. The similarity of the effect for each metal, and the observed 1:1 (L:M) stoichiometry, suggests a common binding mode, in which the aliphatic nitrogens on both pendants bind simultaneously to the metal, leading to a "clamp" structure that restricts the rotation between the rings of the biphenyl unit, in a similar way to a hydrogen bond. Ligand **2** has an ionisable amidic proton. When no base is present in the medium, ligand **2** behaves in

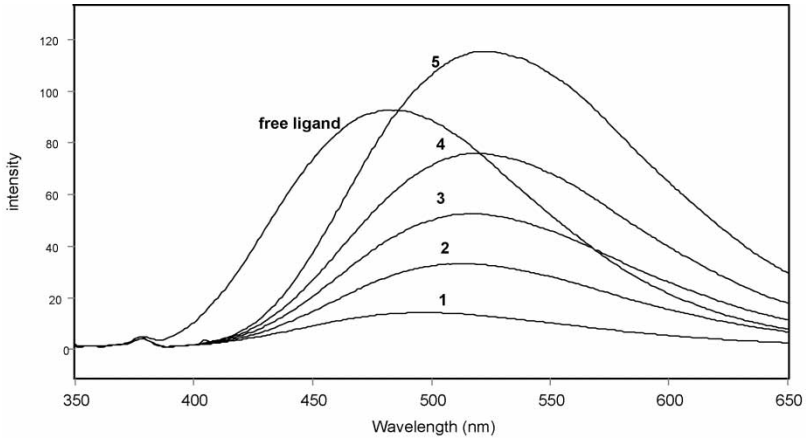

FIGURE 11 Titration of ligand **3** in CH_3CN with Cd^{2+} at 20°C. 1, 2, 3, 4 and 5 indicate the addition of 2.49, 7.47, 12.45, 17.43 and 19.92 equiv. of cadmium triflate, respectively. $\lambda_{exc} = 340$ nm.

a similar way to ligand **1** (with Zn^{2+}) *i.e.*, adopting a clamp conformation, coordinating *via* the amine nitrogens. If a base removes the amidic proton, then a chelating conformation involving both nitrogens on the same branch is preferred, which has no effect on the torsion angle of the biphenyls, and hence no quenching of fluorescence is induced. Ligand **3** displays comparable behaviour with Cu^{2+}, Pb^{2+} and Ni^{2+}, but, with Zn^{2+} and Cd^{2+}, formation of the 1:1 complex is probably followed, at higher metal concentrations, by a more open 1:2 (L:M) complex, in which rotation within the biphenyl unit is no longer hindered, with a consequent restoring of the fluorescence emission intensity.

EXPERIMENTAL SECTION

General Methods

All commercially available reagents were used without further purification. Benzene was dried over sodium. Water sensitive reactions were performed under argon. Column chromatographies were carried out on SDS activated neutral aluminium oxide (0.05–0.2 mm; activity degree 1).

Melting points were measured with a Cambridge Instrument and are uncorrected. IR spectra were recorded on a Perkin-Elmer 1750 FT-IR and a Bruker Equinox 55 FT-IR. NMR spectra were recorded with Bruker Avance 300/500 and Varian Unity-300/400 spectrometers. Chemical shifts are reported in parts per million downfield from TMS. Spectra were referenced to residual undeuterated solvent. High resolution mass spectra were taken with a Fisons VG-AUTOSPEC. UV spectra were run at 20°C (thermostatted) on a on a Biotech Instruments XL spectrometer. Steady-state fluorescence measurements were carried out using an Instruments SA (Jobin-Yvon) Fluoromax-2, equipped with a red sensitive Hamamatsu R928 photomultiplier tube. Spectra were corrected for the wavelength dependence of the detector using a calibration curve generated with a standard lamp.

Fluorescence lifetimes were measured in the frequency domain, using an Instruments S.A. Fluorolog τ-3 instrument, by global fitting of the demodulation and phase shift of the emission, following excitation with sinusoidally-modulated light over the frequency range 10–250 MHz. A suspension of Ludox® in water was used as the standard, which acts as a scattering sample of τ 0.0 ns.

Synthesis of 2-tosyl-5,8-dimethyl-2,5,8-triazanonane (13)

N-Methyl-*N*,*O*-ditosylethanolamine (**12**) (4.16 g, 10.86 mmol) was dissolved in dry acetonitrile (25 ml). NaI (1.76 g, 11.77 mmol) and K_2CO_3 (5.24 g, 37.94 mmol) were added. *N*,*N*,*N*-Trimethylendiamine (1.74 g, 16.48 mmol) was added dropwise and the mixture was refluxed for 24 h. The reaction mixture was filtered and the solvent was evaporated under *vacuum*, to give a dark brown oil. The crude reaction product was purified by chromatography through a silica flash column to give **13** as a brown oil (2.55 g, 8.14 mmol). (75% yield). IR $\bar{\nu}_{max}/cm^{-1}$ (KBr) 2959 (CH), 1597 (C═C), 1465 (CN), 1333 (NSO_2 asym.), 1159 (NSO_2 sym.); ^{1}H NMR (300 MHz, CD_3OD) δ 7.68 (2H, d, $J = 8.4$ Hz, Ar—H), 7.40 (2H, d, $J = 8.4$ Hz, Ar—H), 3.10 (2H, t, $J_1 = 6.8$ Hz, CH_2), 2.74 (3H, s, CH_3), 2.56 (2H, t, $J = 6.8$ Hz, CH_2), 2.54 (2H, t, $J = 4.0$ Hz, CH_2), 2.46 (2H, t, $J = 4.0$ Hz, CH_2), 2.42 (3H, s, CH_3), 2.25 (9H, s, CH_3); ^{13}C NMR (75 MHz, CD_3OD) δ 143.84(s), 134.6 (s), 129.80 (d), 127.48 (d); 56.50 (t), 55.42(t), 54.87 (t), 47.96 (t), 44.74 (q), 41.70 (q), 34.84 (q), 20.48 (q); HRMS (EI): M^+. Found: 313.1778. $C_{15}H_{27}N_3O_2S$ requires 313.1823.

Synthesis of 2,5-dimethyl-2,5,8-triazanonane (6)

2-Tosyl-5,8-dimethyl-2,5,8-triazanonane (**13**) (1.58 g, 5.06 mmol) was stirred, protected by a silica-gel tube, for 72 h at 100°C in concentrated H_2SO_4 (8 ml). The dark obtained solution was dropwise poured into ether. The ethereal layer was separated and the remaining solution was dissolved in H_2O. After addition of NaOH until basic pH it was filtered and extracted with $CHCl_3$. After evaporation of the solvent under reduced pressure, a yellow oil (233.5 mg, 1.46 mmol) (29% yield) was obtained. IR $\bar{\nu}_{max}/cm^{-1}$ (KBr) 3420(NH), 2954 (CH), 1657 (NH), 1466 (CN); ^{1}H NMR (300 MHz, $CDCl_3$) δ 2.33 (2H, t, $J_1 = 6.4$ Hz, CH_2), 2.19 (2H, t, $J = 6.4$ Hz, CH_2), 2.16 (2H, t, $J = 7.6$ Hz, CH_2), 2.12 (3H, s, CH_3), 2.08 (2H, t, $J = 7.6$ Hz, CH_2), 1.93 (3H, s, CH_3), 1.92 (6H, s, CH_3); ^{13}C NMR (75 MHz, $CDCl_3$) δ 55.44 (t), 57.41 (t), 55.90 (t), 49.37 (t), 45.76 (q), 42.61 (q), 36.44 (q); HRMS (CI): $(M^+ + 1)$. Found: 160.1816. $C_8H_{22}N_3$ requires 160.1814.

General Procedure for Synthesis of 4,4′-dinitrobiphenyl Podands

4,4′-Dinitro-2,2′-diphenic acid [17] (0.15 g, 0.45 mmol) was stirred in refluxing $SOCl_2$ (15 ml) for 3 h. After removal of the $SOCl_2$ under *vacuum*and a wash with dry benzene twice, a clear brown oil was obtained. The oil which was dissolved in benzene and added dropwise to a solution of the appropriate amine (**4**, **5**, **6** or diethylamine) (0.96 mmol) in benzene (5 ml), under inert atmosphere. The mixture was stirred for 10 h, giving a solid (**7**, **8**, **9** or **11** respectively), which was filtered, dried under *vacuum* and analysed.

2,2′-Bis(*N, N, N′*-trimethylethylendiaminecarbonyl)-4,4′-dinitrobiphenyl (7)·2 HCl

White powder (64%). IR $\bar{\nu}_{max}/cm^{-1}$ (KBr) 2960 (CH), 2694(N^+H), 1635 (C═O), 1524 (N═O), 1350 (N═O), 1295 (CN); ^1H NMR (300 MHz, CD_3OD) δ 8.57 (2H, d, $J_2 = 1.8$ Hz, Ar—H), 8.45 (2H, dd, $J_1 = 8.4$, $J_2 = 1.8$ Hz, Ar—H), 7.71 (2H, d, $J_1 = 8.4$ Hz, Ar—H), 3.7–3.9 (2H, m, $CONCH_2$) 3.50 (4H, m, CH_2), 3.45-3.25 (2H, m, $CONCH_2$) 2.99 and 2.80 (6H, 2xs, CH_3), 2.94 and 2.91 (12H, 2xs, CH_3); ^{13}C NMR (75 MHz, CD_3OD) δ 169.79 (s), 148.21 (s), 142.14 (s), 136.02 (s), 132.28 (d), 124.58 (d), 122.96 (d), 54.40 (t), 52.86 (t), 42.85 (q), 36.92 (q), 32.81 (q); HRMS (FAB): ($M^+ - H$). Found: 501.2482. $C_{24}H_{33}N_6O_6$ requires 501.2461.

2,2′-Bis(*N, N*-dimethylethylendiaminecarbonyl)-4,4′-dinitrobiphenyl (8)

Brownish powder (65%). IR $\bar{\nu}_{max}/cm^{-1}$ (KBr) 3411 (NH), 3043(CH), 2940 (CH), 1653 (C═O), 1523 (N═O), 1351 (N═O), 833 (CN); ^1H NMR (300 MHz, CD_3CN) δ 8.74 (2H, t, $J = 5.7$ Hz, N—H), 8.55 (2H, d, $J = 2.4$ Hz, Ar—H), 8.32 (2H, dd, $J_1 = 8.7$, $J_2 = 2.4$ Hz, Ar—H), 7.58 (2H, d, $J = 8.7$ Hz, ArH), 3.53 (4H, q, $J = 6$ Hz CH_2), 3.5-3 (4H, m, CH_2), 2.71 (12H, s CH_3); ^{13}C NMR (75 MHz, CD_3OD) δ 168.99 (s), 147.94 (s), 144.00 (s), 136.23 (s), 131.51 (d), 124.90 (d), 122.86 (d), 56.74 (t), 42.91 (q), 35.03 (t); HRMS (EI): ($M^+ - 2H$). Found: 472.2069. $C_{22}H_{28}N_6O_6$ requires 472.2070.

2,2′-Bis(2,5-dimethyl-2,5,8-triazanonanecarbonyl)-4,4′-dinitrobiphenyl (9)

Brownish powder (68%). IR $\bar{\nu}_{max}/cm^{-1}$ (KBr) 2962(alC-H), 2677-2462 (NH^+), 1635 (C═O), 1523 (NO_2), 1348 (NO_2); ^1H NMR (400 MHz, $D_2O + CF_3$-COOH) δ 8.3-8.1 (2H, m, Ar—H), 7.47 (1H, d, $J =$ 7.9 Hz, Ar—H), 7.35 (1H, d, $J = 7.9$ Hz, Ar—H), 7.3-7.1 (2H, m, Ar—H), 3.6-3.1 (16H, 3 × bs, $-CH_2$), 2.9-2.5 (24H, m, $-CH_3$); ^{13}C NMR (100 MHz, $D_2O +$ CF_3COOH) δ 170.03 (s), 167.46 (s), 147.37 (s, 2C), 141.48 (s, 2C), 134.74 (s), 131.33 (s), 131.10 (d), 128.76 (2C, d), 125.36 (d), 125.12 (s), 124.95 (d), 122.98 (d), 53.18 (t), 50.60 (t), 50.54 (t), 43.36 (t), 43.30 (q), 40.58 (q), 40.43 (q), 37.27 (q), 33.21 (q); HRMS (EI): (M^+). Found: 614.3732. $C_{30}H_{46}N_8O_6$ requires 614.3540.

2,2′-Bis(diethylaminecarbonyl)-4,4′-dinitrobiphenyl (11)

Orange powder. (63%). IR $\bar{\nu}_{max}/cm^{-1}$ (KBr) 3096 (arC-H), 2969(alC-H), 2933(alC-H), 1639 (C═O), 1524 (NO_2), 1348 (NO_2), 848(arC-H), 744 (arC-H); ^1H NMR (300 MHz, $CDCl_3$) δ 8.26 (2H, d, $J_2 = 2.1$ Hz, Ar—H), 8.25 (2H, dd, $J_1 = 9.0$, $J_2 = 2.1$ Hz, Ar—H), 7.65-7.55 (2H, bs, Ar—H), 3.35-3.6 (4H, bs, CH_2), 3.35-3.20 (4H, bs, CH_2), 1.2-1.0 (12H, 1 × t ($J = 7.04$ Hz) and 1 bs, CH_3); ^{13}C NMR (75 MHz, $CDCl_3$) δ 167.73 (s), 148.06 (s), 141.73 (s), 139.19 (s), 131.80 (d), 123.83 (d), 122.59 (d), 43.70 (t), 39.63 (t), 14.54 (q), 12.78 (q); HRMS (EI): (M^+). Found: 442.1887. $C_{22}H_{26}N_4O_6$ requires 442.1852.

General Procedure for Synthesis of 4,4′-bis(*N,N*-dimethylamino)biphenyl podands

A heterogenous mixture of the 4,4′-dinitrobiphenyl compound **7**, **8**, **9** (previously deprotonated from their hydrochloride salts by a basic extraction with $NaHCO_3$ and EtOAc) or **11**, (0.527 mmol), formaldehyde (0.2 ml, 37% solution in H_2O) and 10% Pd—C (0.1 g) in absolute ethanol (30 ml) was stirred under H_2 atmosphere (3.4 atm) at room temperature for 36 h. The reaction mixture was filtered, the ethanolic filtrate concentrated and the crude reaction product purified by column chromatography through neutral alumina with CH_2Cl_2:AcOEt (7:3) as eluents, leading to (**1, 2, 3** and **10** respectively).

2,2′-Bis(*N, N, N′*-trimethylethylendiaminecarbonyl)-4,4′-bis(dimethylamine)biphenyl (1)

Green fluorescent cereous solid. (72%) IR $\bar{\nu}_{max}/cm^{-1}$ (KBr) 2952 (CH), 1605 (C═O), 1411 (CN); ^1H NMR (300 MHz, CD_3OD) δ 7.10 (2H, d, $J_1 = 8.4$ Hz, Ar—H), 6.77 (2H, dd, $J_1 = 8.4$, $J_2 = 2.8$ Hz Ar—H), 6.69–6.67 (2H, d, $J_2 = 2.8$ Hz, Ar—H), 3.8–3.4 (2H, bs, $CONCH_2$), 3.30 (2H, m, $CONCH_2$), 2.97 (12H, s, CH_3), 2.91 (6H, bs, CH_3), 2.89 (2H, m, CH_2), 2.47 (2H, m, CH_2), 2.29 (12H, s, CH_3); ^{13}C NMR (75 MHz, CD_3OD) δ 172.85 (s), 149.56 (s), 136.50 (s), 130.83 (s), 124.83 (s), 112.86 (d), 110.47 (d), 56.63 (t), 55.31 (t), 44.57 (q), 39.44 (q), 37.04 (q); HRMS (EI): ($M^+ + 1$). Found: 497.3580: $C_{28}H_{45}N_6O_6$ requires 497.3604.

2,2′-Bis(*N, N*-dimethylethylendiaminecarbonyl)-4,4′-bis(dimethylamine)biphenyl (2)

Green fluorescent cereous solid (68%). IR $\bar{\nu}_{max}/cm^{-1}$ (KBr) 3247 (NH), 2943 (CH), 1639 (C═O), 1602 (C═C), 1495 (CN), 1353 (CN), 810 (arC-H); ^1H NMR (400 MHz, $CDCl_3$) δ 7.69 (2H, t, CON-H), 7.09 (2H, dd, $J_1 = 8.5$, $J_2 = 1.77$ Hz, Ar—H), 6.88 (2H, bs, Ar—H), 6.71 (2H, dd, $J_1 = 8.5$ Hz, Ar—H), 3.7-3.4 (2H, bs, $CONHCH_{A\,B}$), 3.3-3.1 (2H, bs, $CONHCH_{AB}$), 2.98 (12H, s, $ArN(CH_3)_2$), 2.5-2.3 (4H, bs, CH_2), 2.25 (12H, s, CH_3); ^{13}C NMR (100 MHz, $CDCl_3$) δ 171.10 (s), 149.49 (s), 137.25 (s), 131.61 (d), 126.30 (s), 113.25 (d), 110.84 (d), 57.63 (t), 44.49 (q), 40.52 (q), 36.24 (t);

HRMS (EI): (M^+). Found: 468.3275. $C_{26}H_{40}N_6O_2$ requires 468.3213.

2,2′-Bis(2,5-dimethyl-2,5,8-triazanonanecarbonyl)-4,4′-bis(dimethylamine)biphenyl (3)

Green fluorescent cereous solid (73%). IR $\bar{\nu}_{max}/cm^{-1}$ (KBr) 2941 (CH), 1668 (C═O), 1606 (C═C), 1495 (CN), 1354 (CN); ^{1}H NMR (400 MHz, $D_2O + CF_3COOH$) δ 7.62 (2H, d, $J = 2.4$ Hz, Ar—H), 7.62 (2H, dd, $J_1 = 9.23$, $J_2 = 2.4$ Hz, Ar—H), 7.35 (2H, d, $J = 9.23$ Hz, Ar—H), 3.6-3.2 (12H, 2 × bs, CH_2), 3.26 (4H, bs, $CONCH_2$), 3.13 (12H, s, Ar—N $(CH_3)_2$), 2.78 (6H, s, CH_3), 2.76 (12H, s, CH_3), 2.74-2.65 (6H, bs, $CON(CH_3)$); ^{13}C NMR (100 MHz, $D_2O + CF_3COOH$) δ 170.35 (s), 142.33 (s), 137.21 (s), 135.96 (s), 132.56 (d), 122.37 (d), 120.22 (d), 53.19 (t), 50.73 (t), 49.82 (t), 46.33 (t), 43.39 (q), 42.32 (q), 40.60 (q), 39.91 (q), 37.32 (q); HRMS (EI): (M^+). Found: 610.4612. $C_{34}H_{58}N_8O_2$ requires 610.4683.

2,2′-Bis(diethylaminecarbonyl)-4,4′-bis(dimethylamine)biphenyl (10)

White powder (60%). IR $\bar{\nu}_{max}/cm^{-1}$ (KBr) 2966 (arCH), 2928 (alCH), 1630 (C═O), 1608 (C═C), 1486 (CN), 1428 (CN), 809 (arC-H); ^{1}H NMR (500 MHz, $CDCl_3$) δ 7.04 (2H, d, $J_1 = 8.4$ Hz, Ar—H), 6.53 (2H, dd, $J_1 = 8.4$, $J_2 = 2.7$ Hz, Ar—H), 6.49 (2H, d, $J_2 = 2.7$ Hz, Ar—H), 3.8-3.6 (2H, m, CH_{AB}), 3.5-3.3 (2H, m, CH_{CD}), 3.1-2.9 (4H, m, CH_{AB}, CH_{CD}), 2.83 (12H, s, CH_3), 0.97 (6H, t, $J = 7.1$ Hz, $CH_{AB}CH_3$), 0.90 (6H, t, $J = 7.0$ Hz, $CH_{CD}CH_3$); ^{13}C NMR (125 MHz, $CDCl_3$) δ 171.81 (s), 149.32 (s), 137.56 (s), 130.92 (d), 125.06 (s), 112.74 (d), 110.67 (d), 42.89 (t), 40.76 (q), 38.45 (t), 14.13 (q), 12.54 (q); HRMS (EI): (M^+). Found: 438.3013. $C_{26}H_{38}N_4O_2$ requires 38.2995.

X-Ray Diffraction

Crystal Growth

A total of 20.7 mg of **7**·2HCl was dissolved in the minimum volume of methanol and was dropped into a branch of a H-shaped tube. Similarly, 19.5 mg of HgI_2 were placed in the other branch. The tube was carefully filled up with methanol until both branches were connected, and the branches then sealed by a cork stopper. After one month, pale green crystals were obtained in the horizontal branch. They were collected, dried and their X-ray diffraction was measured.

X-ray Crystal Structure Determination of 7

$C_{24}H_{34}Cl_2Hg_2I_4N_6O_6$, $M = 1482.25$, green plate of $0.54 \times 0.23 \times 0.06$ mm size grown by slow liquid–liquid diffusion in methanol, triclinic, space group $P1$, $a = 10.3135(9)$, $b = 11.2280(10)$, $c = 18.8173(15)$ Å, $\alpha = 105.916(7)$, $\beta = 95.243(7)$, $\gamma = 108.559(7)°$, $V = 1948.0(3)$ Å^3, $Z = 2$, $\mu = 11.220$, $2\theta_{max} = 53°$, difractometer Nonius Kappa CCD, Mo-Kα ($\lambda = 0.71073$ Å), ω-scan, $T = 298(2)$ K, 15070 reflections collected of which 7874 were independent, $R_{int} = 0.0747$, direct primary solution and refinement on F^2 using SHELX97 program [18], 397 refined parameters, hydrogen atoms were refined using a *riding* model, $R1[I > 2\sigma(I)] = 0.0693$, $wR2$(all data) = 0.2204.

CCDC-235156 contains the supplementary crystallographic data for this paper. These data can be obtained free of charge at www.ccdc.cam.ac.uk/conts/retrieving.html [or from the Cambridge Crystallographic Data Centre, 12 Union Road, Cambridge CB2 1EZ, UK; fax: (internat.) + 44-1223/336-033; E-mail: deposit@ccdc.cam.ac.uk].

General Procedure for UV Spectra and Fluorimetric Titrations

UV spectra and fluorimetric titrations were carried out in 1 cm pathlength quartz fluorescence cells at 20°C (thermostatted). The concentration of **1**, **2, 3** and **10** was *ca.* 5×10^{-6} M in acetonitrile (spectroscopic grade). An approximately constant ionic strength was maintained by addition of *ca.* 30 mol. of the inert salt $N(Bu)_4PF_6$ per mol of ligand. The measurements were recorded in the presence of Zn(II), Cd(II), Ni(II), Cu(II) and Pb(II) triflates metal-to-ligand ratio between 0.25 to 12 equivalents. For Ni(II), which is known to be extremely slow sometimes, the solution was allowed to equilibrate for up to 2 h and no modification of the emision values with time was observed. Quantum yields were measured using quinine sulphate monohydrate in H_2SO_4 (1 M, aq) as the standard ($\Phi = 0.546$) [19].

Complexation constants were determined from the analysis of the spectral assembly, regarding LM_2, LM and L_2M possible stoichiometries, by fitting the data to each model [20]. Stoichiometric coefficients (n and m) which give more similar values for K_{eq} along the experimental data points in a range of $\alpha = 0.20–0.80$ were chosen to represent the better model.

$$n\,L + m\,M \rightleftarrows L_nM_m$$

$$\alpha = \frac{I - I_0}{I_{lim} - I_0}$$

$$[L] = C_L - n[M_mL_n] = C_L - \alpha C_L = C_L(1 - \alpha)$$

$$[M] = C_M - m[M_mL_n] = C_M - (m/n)\alpha C_L$$

$$K_{eq} = \frac{[M_m L_n]}{[M]^m [L]^n}$$

$$K_{eq} = \left(\frac{C_L^{\frac{n-1}{m}}}{n^{\frac{1}{m}}} \right) \left(\frac{\alpha^{\frac{1}{m}}}{\left(C_M - \frac{m}{n}\alpha C_L\right)(1-\alpha)^{\frac{n}{m}}} \right)^{\frac{1}{2}}$$

where:

C_L : concentration of ligand
C_M: concentration of metal
α : molar fraction of complex
I : analytical signal at each addition (intensity of emission of fluorescence)
I_0 : starting analytical signal value (100% ligand)
I_{lim}: final analytical signal value (100% complex).

Acknowledgements

We acknowledge the support from the Dirección General de Ciencia y Tecnología, project PPQ2002-00986, and from the Agencia Valenciana de Ciencia y Tecnología (IVCiT), for the program Grupos I + D + I, GRUPOS03/206. J.S. thanks the University of Valencia for a predoctoral fellowship.

References

[1] Alkaitis, S. A.; Grätzel, M. *J. Am. Chem. Soc.* **1975**, *98*, 3549.
[2] Mizoguchi, T.; Adams, R. N. *J. Am. Chem. Soc.* **1962**, *84*, 2058.
[3] Seo, E. T.; Nelson, R. F.; Fritsch, J. M.; Marcoux, L. S.; Leedy, R. N. *J. Am. Chem. Soc.* **1966**, *88*, 3498.
[4] Costero, A. M.; Monrabal, E.; Andreu, C.; Martínez-Máñez, R.; Soto, J.; Padilla-Tosta, M.; Pardo, T.; Ochando, L. E.; Amigó, J. M. *J. Chem. Soc., Dalton Trans.* **2000**, 361.
[5] Fritsch, J. M.; Adams, R. N. *J. Chem. Phys.* **1965**, *43*, 1887.
[6] Berlman, I. B. *J. Chem. Phys.* **1970**, *52*, 5616.
[7] Mc Farland, S. A.; Finney, N. S. *J. Am. Chem. Soc.* **2001**, *123*, 1260.
[8] Mc Farland, S. A.; Finney, N. S. *Chem. Commun.* **2003**, 388.
[9] Costero, A. M.; Andreu, R.; Monrabal, E.; Martínez-Máñez, R.; Sancenón, F.; Soto, J. *J. Chem. Soc., Dalton Trans.* **2002**, 1769.
[10] Costero, A. M.; Gil, S.; Sanchis, J.; Peransí, S.; Sanz, V.; Williams, J. A. G. *Tetrahedron* **2004**, *60*, 6327.
[11] Romanelli, M.G.; Becker, E.I. *Org. Synth Coll. V*, 552.
[12] Hope, D. B.; Horncastle, K. C. *J. Chem. Soc. (C)* **1966**, 1098.
[13] Tuladhar, S. M.; D'Silva, C. *Tetrahedron Lett.* **1992**, *33*, 2203.
[14] Bencini, A.; Bianchi, A.; García-España, E.; Fusi, V.; Micheloni, M.; Paoletti, P.; Ramírez, J. A.; Rodríguez, A.; Valtancoli, B. *J. Chem. Soc., Perkin Trans. 2*, **1992**, 1059.
[15] Hashimoto, S.; Thomas, J. K. *J. Chem. Phys.* **1984**, *88*, 4044.
[16] Whitlock, B. J.; Whitlock, H. W. *J. Am. Chem. Soc.* **1990**, *112*, 3910.
[17] Costero, A. M.; Pitarch, M. *Tetrahedron* **1994**, *50*, 5381.
[18] Sheldrick, G. M. *SHELX97*; University of Göttingen: Germany, 1997.
[19] Meech, S. R.; Phillips, D. *J. Photochem.* **1983**, *23*, 193.
[20] Bianchi, A.; Doménech, A.; García-España, E.; Luis, S. V. *Anal. Chem.* **1993**, *65*, 3137.